



Mechanical behaviors and porosity of porous Ti prepared with large-size acicular urea as spacer

Guibao Qiu¹ · Jian Wang¹ · Hao Cui^{2,3} · Tengfei Lu¹

© Springer Nature Switzerland AG 2018

Abstract

Porous Ti scaffolds with average pore size of 600 μm and porosity ranging from 31.1 to 61.2% were successfully prepared by powder metallurgy technology employing large size acicular urea as space holder. Results indicated that the porosity (P) of porous Ti could be determined accurately by added spacer content (S_c) in the green-pressing because the relationship could be formulated as $P = aS_c + b$, where a and b are constants. The compressive strength and structural stiffness were in the range of 50–332 MPa and 0.6–3.7 GPa, respectively. Moreover, the dependence between relative porosity and relative strength, along with the dependence between relative density and relative Yong's modulus were formulated. Our research can provide helpful information to fabricate porous Ti with desirable structure and mechanical properties by spacer method.

Keywords Porosity · Porous Ti · Mechanical behavior

1 Introduction

Porous Ti and its alloys have received considerable attentions in recent years for applications in the field of biomedical engineering such as dental implants and artificial joints due to their unique structure, high chemical resistance and remarkable biocompatibility [1–4]. There are a large number of published reports investigating the preparation and characterization of Ti foams employed in the biomedical industry [5–9]. According to the study of Oh [10], the produced Ti foams with porosity of 30% possess an elastic modulus very close to that of cortical bone. In practical, these novel materials with combined advantages of structural foams and metallic property have many other promising applications. For example, they can be employed as functional materials in terms of heat adsorption given the superior heat conductivity for Ti metal and good energy consumption behavior for foams, if their pore structures are artificially tuned to meet

specific demands [11]. In addition, the applications of Ti based foams in many potential engineering community such as load-bearing sandwich cores in aerospace, naval, and ground transportation industries have already been in focus of attention [12, 13], which requires materials that can work at high temperature or in harsh environment.

Corresponding to different applications, the pore structure including pore size, pore distribution and porosity should be precisely characteristic. Since the space holder technique which can manufacture desirable porous structure without any impurity has been first introduced by Zhao and Sun [14], numerous research have been carried out to prepare porous metal with various spacers such as Mg [15–17], NaCl [18], NH_4HCO_3 [19] and urea [15, 20]. In the work of Lee et al. [21], four types of spacers, namely irregular-shaped urea, spherical urea, sodium chloride, and starch powders, were applied to fabricate porous Ti, and they found that desirable strength and elastic modulus can be obtained by selecting a proper space holder.

✉ Hao Cui, cuihaocqu@163.com | ¹College of Materials Science and Engineering, Chongqing University, Chongqing 400040, China. ²State Key Laboratory of Power Transmission Equipment and System Security and New Technology, Chongqing University, Chongqing 400044, China. ³School of Electrical and Computer Engineering, Georgia Institute of Technology, Atlanta, GA 30332, USA.

Tuncer et al. [22] studied the relationship between porosity of Ti foams and size of spacer, and found that strength and stiffness of products tend to increase with the increasing of pore size. However, they have little investigation on the relationship between mechanical properties of Ti foams and porosity induced by spacer (urea) with large size ($> 1750 \mu\text{m}$). This is important because porous Ti with large pores and relatively high strength can be applied not only as energy adsorbent that can reduce the noise or heat but also as load-bearing sandwich cores in aerospace that can lower weight for supporter. In terms of porous Ti prepared by space holder technology, the porosity is gained by adding needed volume fraction of space holder namely spacer content. Literature [15, 21, 23–27] reported that the porosity might be less than, equal to or greater than spacer content. The main reason of this interesting phenomenon could be attributed to the decreased volume of macro-pores is larger, equal or less than increased volume of micro-pores during sintering. But once the large size spacer is employed to prepare foams, the volume of micro pores would be reduced to a large extent, leading to the obtained porosity more desirable and related mechanical behavior much closer to what the manufacturer want. Therefore, the relationship should be further clarified.

This work attempts to shed light on the effect of large size spacer on porosity and mechanical behaviors of prepared porous Ti, with the size of space holder over $1750 \mu\text{m}$. Compared with other spacers, urea has the advantages of rapid dissociation, easy removal, little residual and low cost, thus it is selected as the space holder in our work. Our experiment would be meaningful not only lying in the systemically analyzed the effect of this urea on the porosity and mechanical properties for obtained Ti foams, but also giving a supplement for predicting these parameters of Ti foams prepared by spacer method.

2 Materials and methods

Due to the high affinity to atmospheric gases, porous Ti were prepared in this study by powder metallurgy method, which can offer a high degree of freedom to produce structures in a wide range. The purchased Ti powder has the purity $> 99.5\%$ and powder size of 300 meshes, with the chemical components by mass percentage listed in Table 1.

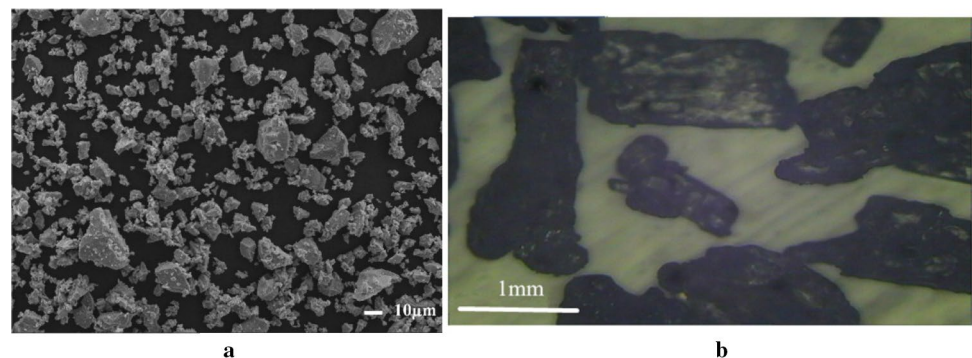
The commercial acicular urea has the average particle size of 2 mm with content of $\text{CO}(\text{NH}_2)_2 > 99\%$, indicating that the spacer can be removed with little impurity. One thing should be noted that the Ti powders were pretreated by the high energy ball-milling machine for 25 min in order to reduce the particle size and simultaneously improve the fluidity between powders.

Figure 1 shows the geometries of raw materials. In Fig. 1a where the morphologies of the Ti powders is shown, it can be observed that the Ti powder size generally gets reduced, smaller than $50 \mu\text{m}$ to a large extent due to the milling process. Based on our previous research, we found that the smaller powder size of Ti can contribute to the compressing, making the process much easier, namely helping to obtain related green-sample more integrate compared with those compressed by untreated powder which are readily to be ruptured. Through milling, not only the powder size can be lowered, but also the improved surface energy can be provided in terms of Ti powder, which makes it more activated. In this case, the bulk of powder would be much easier to be a whole green body under the external stress [28]. In Fig. 1b, we can found that the size of urea particles are basically larger than $1750 \mu\text{m}$ according to the icon inner the figure, which is in agreement with our research aim.

Table 1 Chemical components of commercial Ti power

Components	Si	Fe	Cl	C	O	N	H
Content (%)	0.03	0.05	0.03	0.02	0.32	0.01	0.04

Fig. 1 Micrographs of raw powders **a** Ti powder and **b** urea particle



For compression, the cylindrical specimens were of a height to width ratio of between 1.5 and 2.0 according to the draft standard ISO/DIS 13314 "Compression Test for Porous and Cellular Metals" [29]. Therefore, the size of green-sample was defined as a cylinder with radius of 7.5 mm and height of 12 mm, thus the volume of Ti foam would be 1846.32 mm³, in which the volume of urea were added to be 30%, 40%, 50%, and 60%, respectively. Then, Ti powder and urea were mixed together for 20 min to ensure homogenous distribution of Ti powders on urea particles. Varying amount of Ti and urea added in green compacts is based on the following relation:

$$\frac{W_{Ti}}{W_{urea}} = \frac{\rho_{Ti} \cdot (1 - V_{urea})}{\rho_{urea} \cdot V_{urea}} \quad (1)$$

where the W represents the mass of raw materials, ρ and V are density of volume of raw materials respectively. Subsequently, a little alcohol (about 0.5 ml) and zinc stearate (about 0.5 g) was added into the mixture to improve the fluency and lubrication property between the particles and the cylindrical die. After the mixing particles were decanted into the compress die, they are then uniaxially compressed into a green compact under a constant pressure of 200 MPa for 1 min to ensure the uniform pressing that samples suffered. The final step upon these so-prepared green compacts for obtaining the products of Ti foam is sintering, which is divided into two stages for different aims. During the heating process, the samples were heated up to 400 °C firstly at a constant heating rate of 10 °C per minute to initially remove the spacer of urea. The temperature should keep at the point of 400 °C for 40 min, to guarantee the complete decomposition of the urea and the thorough removal of its decomposed components. Secondly, at the sintering temperature of 1250 °C, the samples were fritted for 2 h. It should be noted that the sintering point, duration time and pressure mentioned above were demonstrated sufficiently in our previous studies [30]. In that case, we can make a comparison among different properties of porous Ti in the same preparing conditions. In addition, due to the active performance of Ti in the surrounding at high temperature [31], the high-purity argon ($\geq 99.99\%$) was poured into the sintering chamber during the whole process to achieve the atmosphere requirements and remove potential trace

oxygen surrounding samples. Finally, the samples were taken out from the furnace after they have been cooled to ambient temperature.

The pore structures of Ti foams were characterized by scanning electron microscope (SEM), while the porosity calculated according to the following equation [32, 33]:

$$P = 1 - \frac{\rho^*}{\rho_s} \quad (2)$$

where ρ^* represents the density of porous Ti, which can be measured by dividing the whole weight to the whole volume of the sample, whereas ρ_s denotes the density of the solid Ti ($\rho_s = 4.503 \text{ g/cm}^3$).

To investigate the compressive behavior, the obtained foams were compressed by a Universal Testing Machine at a displacement rate of 1 mm/min to guarantee a stable stress transfer through the pressuring samples. All the compression processes are performed through the longitudinal direction. Considering the reliability of compression data and repeatability of experiment, the porosity, compressive strength and structural stiffness were finally determined by calculating the average value of five samples.

3 Results and discussion

In the present work, porous Ti with porosity ranging from 31.1% to 61.2% and main pore size of 600 μm was produced by spacer method, with different volume fraction of urea added to determine the obtained porosity. In addition, the mixture ratio for Ti and spacer, porosity and the compressive results of obtained products are exhibited in Table 2.

Based on this table, one can find that the porosity of forms witnesses a rising tendency with the increasing content of added spacer from 30 to 60%, and the values for calculated porosities are all larger than those of added volume of spacer, which will be further analyzed in the following section. On the other hand, the compressive strength along with the density of obtained products are decreased sharply as the increasing content of urea. This is understandable because if the adding content of spacer becomes larger, the volume fraction for pores would get

Table 2 Mixture ratio, porosity and compressive data of porous Ti

Sample	Mixture ratio	Density (g/cm ³)	Porosity (%)	Strength (MPa)	Stiffness (GPa)
Ti/AU	7:3	3.10±0.04	31.1±0.8	331.84±7.5	3.69±0.08
	6:4	2.66±0.01	40.9±0.2	193.25±6.6	2.87±0.10
	5:5	2.19±0.05	51.3±1.1	108.67±4.2	1.68±0.06
	4:6	1.75±0.03	61.2±0.6	50.34±3.3	0.64±0.04

large accordingly after sintering, thereby leading to the plummet in material density and strength. Detailed analysis would be mentioned in the following sections.

3.1 Pore structural analyses

In the urea removal stage, the decomposed species of urea have been completely sublimated under the temperature of 400 °C, forming pores at places where the urea particles were stayed. After that, in the sintering process, the pore structure would be dramatically affected due to the thermal stress induced by the heating process. Figure 2 exhibits the pore structure of Ti foams with different size and property.

It has been reported [34] that pores in porous metals could be divided into two types: the micro-pores and the macro-pores. The former is generated due to the partial sintering of Ti powers on the sidewall of pores, which frequently has the size only several micrometers (in Fig. 2a). On the other hand, the latter that has much larger size are obtained by the decomposition of spacer particles. To meet the requirement of practical applications, the kinds of macro-pores should be distinguished as well. The first type is unconnected pores as depicted in Fig. 2b, in which the pores stand individually and solely due to the homogeneous distribution of a small fraction of urea particles on Ti powers. In other words, this kind of pores are likely to be formed in the foams with small porosity lower than 30%. Whereas, the second one is called interconnected pores as seen in Fig. 2c, which are formed because of the large fraction of spacer in a form, leading to a large number of vacancies after sintering. This pores are also named opening pores, which usually can be found in a high porosity foam larger than 50%.

The pore size and distribution of prepared Ti foams are described in Fig. 3. One can conclude based on this figure that the pore size spans in the range of 300–1000 μm, which is smaller than the added spacer size due to the shrinkage of the pores during the sintering process at high

temperature. Simultaneously, with the increase of porosity, the pore distribution becomes denser and denser, up to a point that pores are basically connected within only a little Ti support in the foam with porosity of 60%. This structure would be favorable for a Ti foam being produced as energy adsorbent for noise and heat consumption, or as promising candidate for hollow plate layer given its combined advantages of light weight and high heat resistance.

3.2 Dependence between porosity and spacer content

It is well-known that the porosity of foams prepared by powder metallurgic technology is dependent on many factors such as spacer type, volume and size, pressure for a green-pressing, sintering temperature, etc. The spacer volume, however, plays the most significant role among all factors confirmed by the Ref. [35], where a linear relationship between porosity (P) and added spacer content (S_c) was demonstrated. This implies that the other parameter for porous Ti preparation would not exert dramatic influence towards the relationship between P and S_c . Plotted in Fig. 4 is such linear relationship obtained according to our results, although the large size spacer was employed in the present work. Therefore, in accordance with the previous report, we assume that the so-called porosity model equation for porous Ti prepared by spacer method would be formulated as $P = aS_c + b$, with a and b to be 1.0072 and 0.7255, respectively, in our work.

Therefore, the equation here can be obtained as $P = 1.0072S_c + 0.7255$ ($R^2 = 0.99975$). It is explicit based on this equation that the porosity of porous Ti prepared by acicular urea with large size would be larger than spacer content. This phenomenon can also be explained by the Gibbs free energy model regarding the sintering potential developed by Cocks [36], expressed as:

$$dG = (\gamma_s - \gamma_b/2)dA - \sum_m dV = \gamma_s(1 - \cos \theta)dA - \sum_m dV \quad (3)$$

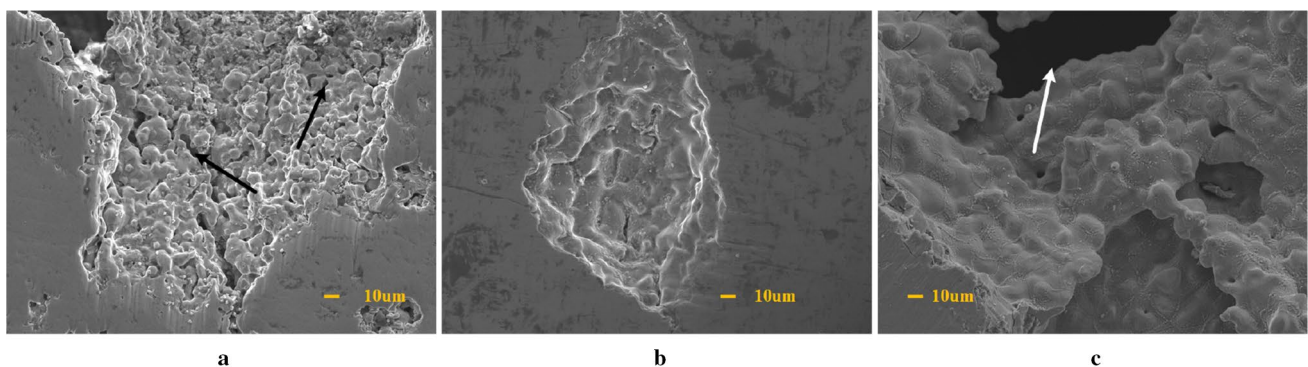


Fig. 2 SEM patterns of porous Ti: **a** micro pores; **b** unconnected pores; **c** interconnected pores

Fig. 3 Pore distributions of cross profile in foams with porosity varying from 30 to 60%

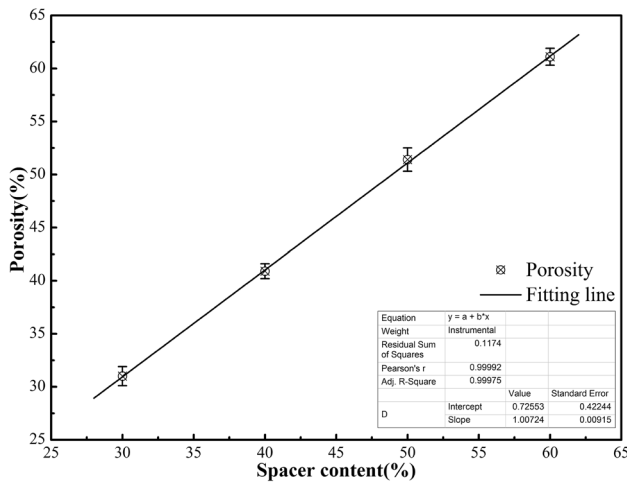
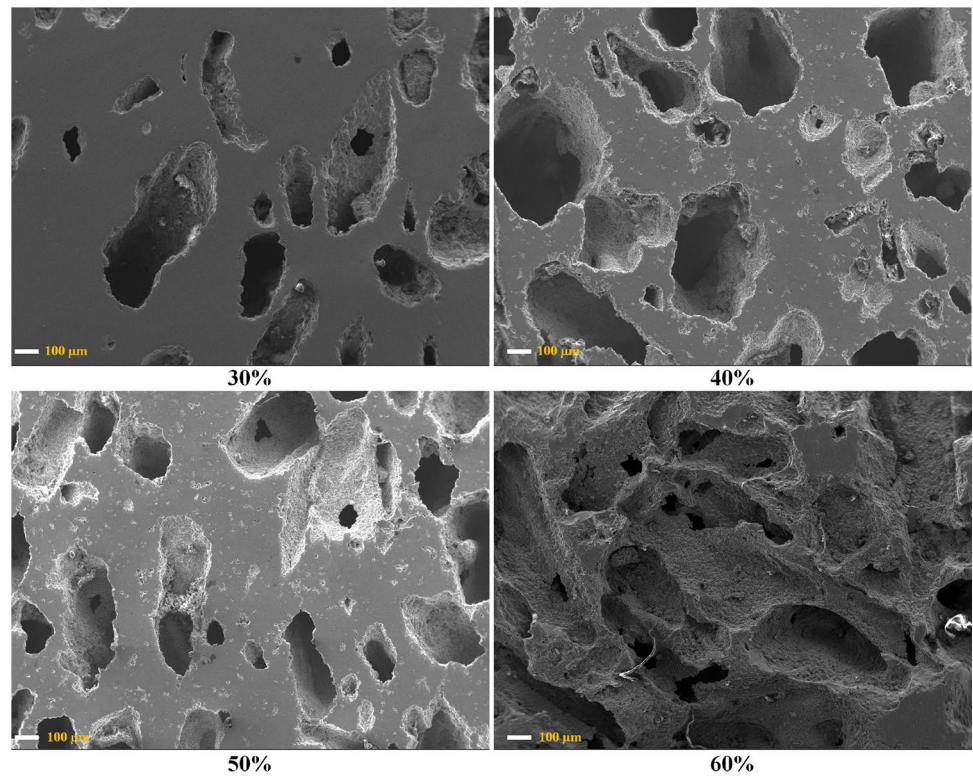


Fig. 4 Relationship between porosity and spacer content

$$\cos \theta = \gamma_b / 2\gamma_s \tag{4}$$

where γ_s is the surface energy, γ_b is the grain-boundary energy, Σ_m is the mean stress, while dA and dV represent the changes in the surface area and pore volume, respectively. Considering the stick-like spacer shape used in this work, Eq. 3 can be rewritten as follows, with the underlying assumption that the formed pores inner the samples can be approximately presumed as cylinders.

$$dG = \left[\frac{\gamma_s \cdot (1 - \cos \theta) \cdot r \cdot h}{2(r + h)} - \Sigma_m \right] dV = \left[\Sigma_s - \Sigma_m \right] dV \tag{5}$$

where r is the pore radius, h is the pore height and Σ_s is the sintering potential. The r of urea is similar in this study owing to the griddle of a 10 meshes sifter for its pre-selection. Based on Eq. 5 we can find that the increasing pore height would reduce the sintering potential at a constant temperature and thus retard the sintering rate. In the meanwhile, it has been investigated that pores inner foams with volume larger than 0.5 mm^3 will induce the decrease of sintering potential and density [37]. The pores here caused by large size urea are evidently larger than 1 mm^3 , which would not only lower the sintering rate, but also reduce the density of products, thereby leading to the huge porosity for foams. Moreover, it should be mentioned that the large pores inner the samples could also hinder the condensation of Ti powders, weakening the binding and sintering between Ti powers as well, which is another contributor lowering the foam density. Combined the overall analysis above, there would be no doubt that the obtained porosity of our specimens are higher than the added spacer content.

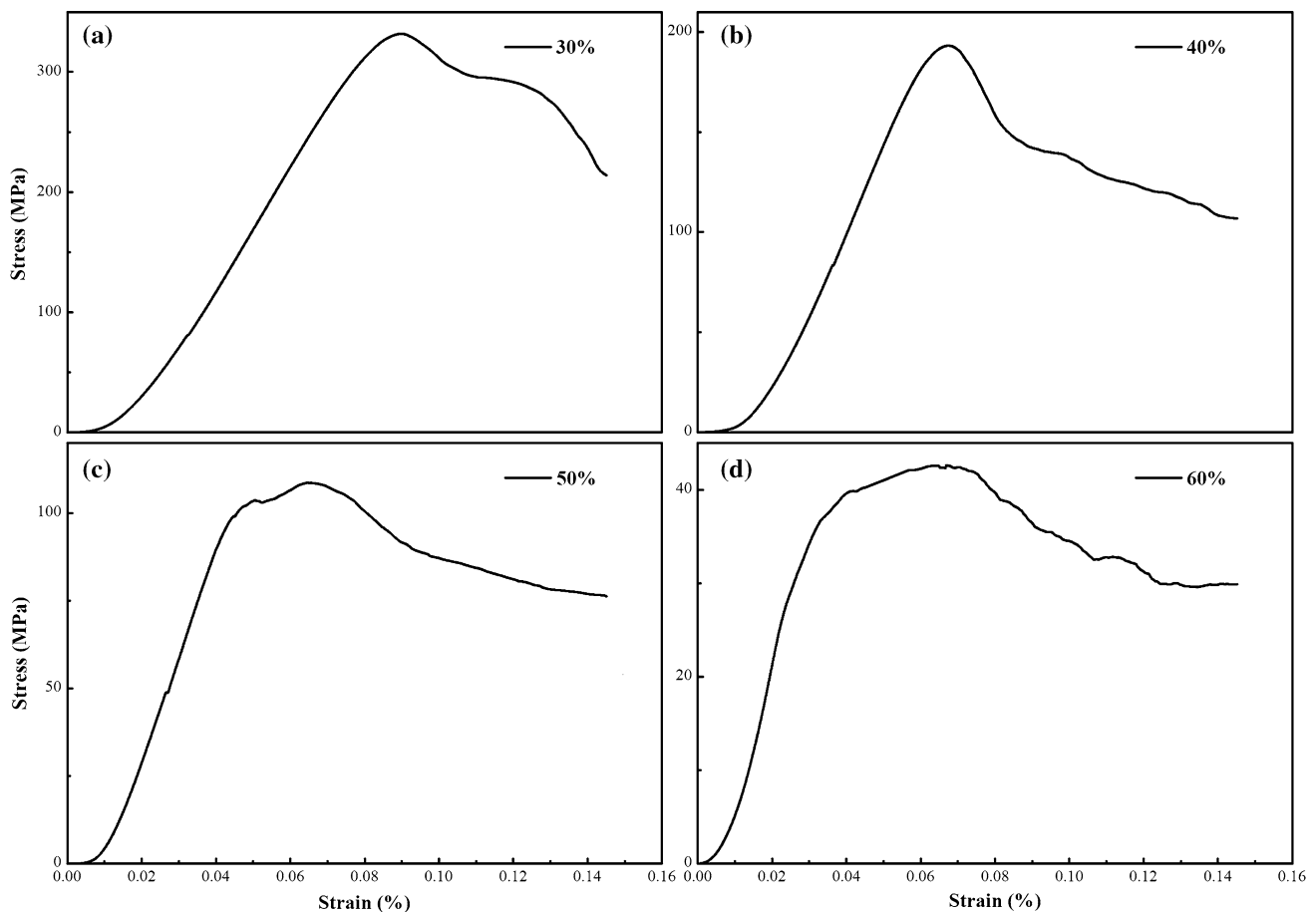


Fig. 5 Stress–strain curves of porous Ti with different porosities

3.3 Mechanical behaviors analyses

The compressive stress–strain curves of Ti foams depending on the spacer fraction are shown in Fig. 5.

The previous discussions in the basis of Table 2 have concluded that both compressive strength and structural stiffness are showed a continuous decrease as the porosity increased, and here we give some detailed expressions. It has been reported [16, 38] that the stress–strain curves exhibits three distinct regions in the compressing process: (1) linear elastic region, (2) plateau region, and (3) densified region. In the plateau region, stress oscillates around an average stress value and remains relatively flat even with increase in strain value (the average stress in this region is termed as plateau stress). In densified region, stress increased drastically with slight increase in strain. In this work, the compressive stress–strain curves are presented in a similar way, although ill-defined densified regions. From Fig. 5, one can deduce that with the increase of porosity, not only the compressive stress becomes gradually decrease, but

related strains drop when the stress grows up to the largest. This could be attributed to the increasing porosity with large pore size of average 600 μm induced by the large size of acicular urea in the foams. In other words, these formed large pores are likely to be collapsed in the compression process, thus accelerating the linear elastic region to a large extent. Apart from that, stable plateau regions can be found when the foams suffered the compressive strength. This is in agreement with the property for porous material, which can be explained by the uniform stress undergone by the foams with the gradually collapsed pores if the prepared foams possess the homogenous pore structure. In the third region, the compacting specimens were completely collapsed and crumbled into a pitch of small foams, instead of a dense bulk. This would be the reason why there has no evident densified region of our prepared specimens during compression. In practical, the behavior of stress–strain curve is closely related to the property of the spacer holder; while the main purpose of this work is to investigate the effect of large size spacer on the porosity and

mechanical properties of Ti foams. In this regard, one could comprehend that these large size of pores are vulnerable to be crushed once the compacting stress is beyond their topmost strength, resulting in the breakage of Ti walls between pores, and then collapsing the foams. Even so, these materials possessing relatively high strength and good yield performance would be suitable for energy cushioning and consuming material given their uniform distribution of pore structure.

In the previous research, number empirical formulas were proposed to characterize and predict the mechanical properties of porous Ti, revealing the relations between compressive strength associated with structural stiffness of foams and related density. All the theoretical models, frankly speaking, are based on some idealized microstructures, e.g. uniform spherical, cylindrical or cubic pores arranged in a cubic array, and therefore the derived correlations between properties and porosity cannot usually be extended directly to real materials with pores of irregular shapes, non-uniform size and random distribution [15]. Gibson and Ashby [39] raised a model to represent the strength of cellular solids, which shows a linear dependence between structural stiffness and the relative density term (ρ^*/ρ_s). Another model introduced by Esen and Bor [17] indicated that the relationships between the strength and relative density in parallel with the structural stiffness and the relative density of porous Ti obey a power law relation, shown as:

$$E^*/E_s = A(\rho^*/\rho_s)^B \tag{6}$$

$$\sigma^*/\sigma_s = C(\rho^*/\rho_s)^D \tag{7}$$

where E , σ and ρ represent structural stiffness, compressive stress, and density, respectively, and the other factors are empirical constants. Furthermore, the superscript * and the subscript s represent the corresponding values of porous and bulk materials, respectively. In the present work, the values were adopted as $E_s = 104.1$ GPa, $\sigma_s = 485$ MPa, and $\rho_s = 4.503$ g/cm³ [40].

However, these relationships can be changed according to variation of experimental condition and parameter determination, including raw materials, processing condition as well as sintering parameters. Our results is no exception. As shown in Figs. 6 and 7, the relative stiffness (E^*/E_s) of a foam is well described as a linear dependence on porosity ($P = 1 - \rho^*/\rho_s$), a conclusion that accords with that reported by Tuncer [41]; while the relationship between relative compressive strength and relative density fits properly with Eq. (2). Summly, the equation to illustrate the relationship between porosity and stiffness could be formulated as $E^*/E_s = 0.067 - 9.92 \times 10^{-2} P$; on the other hand, the relationship between relative strength and

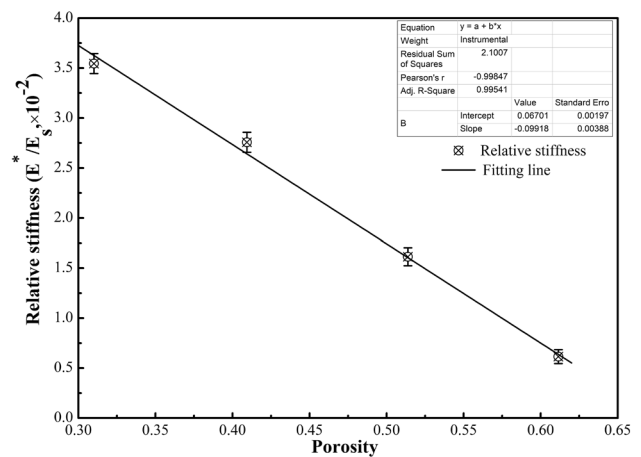


Fig. 6 Relationship between porosity and relative structural stiffness

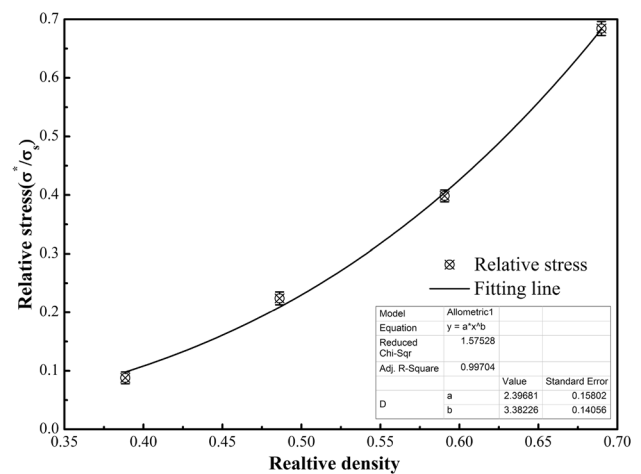


Fig. 7 Relationship between relative density and relative strength

relative density could be expressed as $\sigma^*/\sigma_s = 2.397 \times (\rho^*/\rho_s)^{3.38}$.

After obtaining these two formulations, it would be more comprehensive to understand the porosity and mechanical properties of Ti foam prepared by urea, through analyzing the effect of large size urea on these parameters. In addition, it would be more convenient to predict the physical properties of Ti foams prepared by spacer method.

4 Conclusions

To enhance the investigation of spacer effect on porosity and mechanical properties for prepared Ti foams by spacer method, the large size urea particles were employed as space holder in the present work. The main conclusions are as follows:

1. The porosity, compressive strength, and structural stiffness for obtained foams are in the range of 31.1–61.2%, 50–322 MPa and 0.6–3.7 GPa, respectively.
2. The average pore size of 600 μm is generated and distributed uniformly inner the foams.
3. The relationship between porosity (P) and spacer content (S_c) is formulated by $P = 1.007S_c + 0.7255$, which is helpful to obtain certain porosity of a foam by removal of the spacer.
4. Additionally, the relation between relative compressive strength and density obeys a power law relation; while the relationship between relative stiffness and porosity are described as a linear dependence. In this way, the mechanical properties of foams could be predicted by the models when using the space holder technology.

Acknowledgements This study was supported by the Fundamental Research Funds for the Central Universities (No. 106112017CDJPT130004) and by the Natural Science Foundation of China (No. 51174243) and (No. 51674055).

Author contributions GQ conceived and designed the research, HC performed the research and wrote this manuscript while JW and TL helped analyze the data. GQ and HC contribute equally towards this work.

Compliance with ethical standards

Conflict of interest The authors declare no conflict of interest.

References

1. Niinomi M (2002) Recent metallic materials for biomedical applications. *Metall Mater Trans A* 3:477–486
2. Greiner C, Oppenheimer SM, Dunand DC (2005) High strength, low stiffness, porous NiTi with superelastic properties. *Acta Biomater* 6:705–716
3. Spoerke ED, Murray NG, Li H, Brinson LC, Dunand DC, Stupp SI (2005) A bioactive titanium foam scaffold for bone repair. *Acta Biomater* 5:523–533
4. Geetha M (2009) Ti based biomaterials, the ultimate choice for orthopaedic implants—a review. *Prog Mater Sci* 3:397–425
5. Chen YJ, Feng B, Zhu YP, Weng J, Wang JX, Lu X (2009) Fabrication of porous titanium implants with biomechanical compatibility. *Mater Lett* 63(30):2659–2661
6. Fukuda A, Takemoto M, Saito T, Fujibayashi S, Neo M, Pattanayak DK, Matsushita T, Sasaki K, Nishida N, Kokubo T (2011) Osteoinduction of porous Ti implants with a channel structure fabricated by selective laser melting. *Acta Biomater* 7(5):2327–2336
7. Takemoto M, Fujibayashi S, Neo M, Suzuki J, Matsushita T, Kokubo T, Nakamura T (2006) Osteoinductive porous titanium implants: effect of sodium removal by dilute HCl treatment. *Biomaterials* 27(13):2682–2691
8. Torres Y, Pavón JJ, Rodríguez JA (2012) Processing and characterization of porous titanium for implants by using NaCl as space holder. *J Mater Process Technol* 212(5):1061–1069
9. Yang YZ, Tian JM, Tian JT, Chen ZQ, Deng XJ, Zhang DH (2000) Preparation of graded porous titanium coatings on titanium implant materials by plasma spraying. *J Biomed Mater Res* 52(52):333–337
10. Oh I-H, Nomura N, Masahashi N, Hanada S (2003) Mechanical properties of porous titanium compacts prepared by powder sintering. *Scr Mater* 49(12):1197–1202
11. Stephani G, Quadbeck P, Andersen O (2009) New multifunctional lightweight materials based on cellular metals—manufacturing, properties and applications. *J Phys Conf Ser* 165(2009):012061
12. Banhart J (2001) Manufacture, characterization and application of cellular metals and metal foams. *Prog Mater Sci* 6:559–632
13. Salimon A, Bréchet Y, Ashby MF, Greer AL (2005) Potential applications for steel and titanium metal foams. *J Mater Sci* 22:5793–5799
14. Zhao YY, Sun DX (2001) A novel sintering-dissolution process for manufacturing Al foams. *Scr Mater* 44(1):105–110
15. Niu W, Bai C, Qiu G, Wang Q (2009) Processing and properties of porous titanium using space holder technique. *Mater Sci Eng A* 506(1–2):148–151
16. Aydoğmuş T, Bor Ş (2009) Processing of porous TiNi alloys using magnesium as space holder. *J Alloys Compd* 478(1–2):705–710
17. Esen Z, Bor Ş (2007) Processing of titanium foams using magnesium spacer particles. *Scr Mater* 56(5):341–344
18. Ye B, Dunand DC (2010) Titanium foams produced by solid-state replication of NaCl powders. *Mater Sci Eng A* 528(2):691–697
19. Xu JL, Bao LZ, Liu AH, Jin XJ, Tong YX, Luo JM, Zhong ZC, Zheng YF (2015) Microstructure, mechanical properties and superelasticity of biomedical porous NiTi alloy prepared by microwave sintering. *Mater Sci Eng C* 46:387–393
20. Wen CE, Mabuchi M, Yamada Y, Shimojima K, Chino Y, Asahina T (2001) Processing of biocompatible porous Ti and Mg. *Scr Mater* 45(10):1147–1153
21. Lee B, Lee T, Lee Y, Dong JL, Jeong J, Yuh J, Sang HO, Kim HS, Chong SL (2014) Space-holder effect on designing pore structure and determining mechanical properties in porous titanium. *Mater Des* 57(57):712–718
22. Tuncer N, Arslan G, Maire E, Salvo L (2011) Investigation of spacer size effect on architecture and mechanical properties of porous titanium. *Mater Sci Eng A* 530(1):633–642
23. Bansiddhi A, Dunand DC (2007) Shape-memory NiTi foams produced by solid-state replication with NaF. *Intermetallics* 15(12):1612–1622
24. Jha N, Mondal DP, Dutta Majumdar J, Badkul A, Jha AK, Khare AK (2013) Highly porous open cell Ti-foam using NaCl as temporary space holder through powder metallurgy route. *Mater Des* 47:810–819
25. Hong TF, Guo ZX, Yang R (2008) Fabrication of porous titanium scaffold materials by a fugitive filler method. *J Mater Sci Mater Med* 19(12):3489–3495
26. Chino Y, Dunand DC (2009) Creating aligned, elongated pores in titanium foams by swaging of preforms with ductile space-holder. *Adv Eng Mater* 11(1–2):52–55

27. Torres Y, Rodríguez JA, Arias S, Echeverry M, Robledo S, Amigo V, Pavón JJ (2012) Processing, characterization and biological testing of porous titanium obtained by space-holder technique. *J Mater Sci* 47(18):6565–6576
28. Kim SW, Jung HD, Kang MH, Kim HE, Koh YH, Estrin Y (2013) Fabrication of porous titanium scaffold with controlled porous structure and net-shape using magnesium as spacer. *Mater Sci Eng C Mater Biol Appl* 33(5):2808–2815
29. Technical Committee ISO/TC 164 (2011) Compression test for porous and cellular metals-ISO 13314
30. Xiao J, Qiu G, Liao Y, Bai C (2015) Microstructure and mechanical properties of titanium foams prepared with carbamide as space holder. *Rare Metal Mater Eng* 44(7):1724–1729
31. Jiang G, Li Q, Wang C, Dong J, He G (2015) Fabrication of graded porous titanium–magnesium composite for load-bearing biomedical applications. *Mater Des* 67:354–359
32. Hu Y, Grainger DW, Winn SR, Hollinger JO (2002) Fabrication of poly(α -hydroxy acid) foam scaffolds using multiple solvent systems. *J Biomed Mater Res* 59(3):563–572
33. Maspero FA, Ruffieux K, Müller B, Wintermantel E (2002) Resorbable defect analog PLGA scaffolds using CO₂ as solvent: structural characterization. *J Biomed Mater Res* 62(1):89–98
34. Lewis (2013) Properties of open-cell porous metals and alloys for orthopaedic applications. *J Mater Sci Mater Med* 24(10):2293–2325
35. Jian X, Hao C, Guibao Q, Yang Y, Xuwei L (2015) Investigation on relationship between porosity and spacer content of titanium foams. *Mater Des* 88:132–137
36. Cocks ACF (2001) Constitutive modelling of powder compaction and sintering. *Prog Mater Sci* 46(3–4):201–229
37. Lee B, Lee T, Lee Y, Lee DJ, Jeong J, Yuh J, Oh SH, Kim HS, Lee CS (2014) Space-holder effect on designing pore structure and determining mechanical properties in porous titanium. *Mater Des* 57:712–718
38. Mansourighasri A, Muhamad N, Sulong AB (2012) Processing titanium foams using tapioca starch as a space holder. *J Mater Process Technol* 212(1):83–89
39. Wolcott MP (1990) Cellular solids: structure and properties. *Mater Sci Eng A* 123(2):282–283
40. Niinomi M (1998) Mechanical properties of biomedical titanium alloys. *Mater Sci Eng A* 243(1–2):231–236
41. Tuncer N, Arslan G (2009) Designing compressive properties of titanium foams. *J Mater Sci* 44(6):1477–1484